ARTICLE
Journal of Cellular Biochemistry 115:540–548 (2014)

Journal of Cellular Biochemistry

Nanotopography Drives Stem Cell Fate Toward Osteoblast Differentiation Through α1β1 Integrin Signaling Pathway

A.L. Rosa,[1] R.B. Kato,[1] L.M.S. Castro Raucci,[1] L.N. Teixeira,[1] F.S. de Oliveira,[1] L.S. Bellesini,[1] P.T. de Oliveira,[1] M.Q. Hassan,[2] and M.M. Beloti[1]*

[1]*Cell Culture Laboratory, School of Dentistry of Ribeirão Preto, University of São Paulo, Av do Café s/n, 14040-904, Ribeirão Preto, SP, Brazil*

[2]*Department of Oral and Maxillofacial Surgery, School of Dentistry, University of Alabama at Birmingham, 1919 7th Avenue South, Birmingham, Alabama 35294*

ABSTRACT

The aim of our study was to investigate the osteoinductive potential of a titanium (Ti) surface with nanotopography, using mesenchymal stem cells (MSCs) and the mechanism involved in this phenomenon. Polished Ti discs were chemically treated with H_2SO_4/H_2O_2 to yield nanotopography and rat MSCs were cultured under osteogenic and non-osteogenic conditions on both nanotopography and untreated polished (control) Ti surfaces. The nanotopography increased cell proliferation and alkaline phosphatase (Alp) activity and upregulated the gene expression of key bone markers of cells grown under both osteogenic and non-osteogenic conditions. Additionally, the gene expression of α1 and β1 integrins was higher in cells grown on Ti with nanotopography under non-osteogeneic condition compared with control Ti surface. The higher gene expression of bone markers and Alp activity induced by Ti with nanotopography was reduced by obtustatin, an α1β1 integrin inhibitor. These results indicate that α1β1 integrin signaling pathway determines the osteoinductive effect of nanotopography on MSCs. This finding highlights a novel mechanism involved in nanosurface-mediated MSCs fate and may contribute to the development of new surface modifications aiming to accelerate and/or enhance the process of osseointegration. J. Cell. Biochem. 115: 540–548, 2014.

KEY WORDS: INTEGRIN; MESENCHYMAL STEM CELL; NANOTOPOGRAPHY; OSTEOBLAST; TITANIUM

In the field of implantology research tremendous efforts have been employed to achieve enhanced and high quality physiological osseointegration, mainly in demanding bone sites. Recent sightings have highlighted that nanotechnology is a powerful tool, which modulates the osteoblast responses to titanium (Ti) implant surfaces, directly affecting the process of osseointegration [Mendonça et al., 2010; Bueno et al., 2011; Dimitrievska et al., 2011; Menon et al., 2012; Gittens et al., 2013]. It has been demonstrated that distinct patterns of nanotopography, either ordered or disordered, dramatically regulate the osteoblastic cell activity from adhesion until extracellular matrix mineralization [Ward and Webster, 2006; de Oliveira et al., 2007; Divya et al., 2009; Vetrone et al., 2009; Raimondo et al., 2010]. Nanocoating Ti with either TiO_2, ZrO_2 or Al_2O_3 as well as H_2SO_4/H_2O_2 treatment have produced surfaces that upregulate a set of key modulators of the osteoblast phenotype in human mesenchymal stem cells (MSCs) [Mendonça et al., 2009, 2010].

The Ti with nanotopography surfaces produced by a controlled chemical oxidation using a mixture of H_2SO_4/H_2O_2 have been extensively characterized in terms of physical structure and surface chemistry [Yi et al., 2006; Variola et al., 2008]. In addition to produce an unique topography presenting nanopits with an average size of 22 nm and a threefold increase in surface roughness, this chemical treatment increases the thickness of the TiO_2 layer from ~5 nm to ~32–40 nm and reduces the presence of contaminants such as N and Si compared with an untreated Ti surface [Yi et al., 2006]. Moreover, the X-ray diffraction patterns of Ti with nanotopography and untreated Ti surfaces did not show any anatase or rutile peaks, suggesting that both surfaces are amorphous [Yi et al., 2006].

The authors declare that they have no conflict of interest.

Grant sponsor: State of São Paulo Research Foundation (FAPESP, Brazil); Grant numbers: 2010/18395-3, 2010/19280-5; Grant sponsor: National Council for Scientific and Technological Development (CNPq, Brazil); Grant number: 301023/2010-7.

*Correspondence to: Marcio M. Beloti, Cell Culture Laboratory, School of Dentistry of Ribeirão Preto, University of São Paulo Av do Café s/n, 14040-904 Ribeirão Preto, SP, Brazil. E-mail: mmbeloti@usp.br

Manuscript Received: 13 June 2013; Manuscript Accepted: 26 September 2013

Accepted manuscript online in Wiley Online Library (wileyonlinelibrary.com): 5 October 2013

DOI 10.1002/jcb.24688 • © 2013 Wiley Periodicals, Inc.

Our group has been investigating many aspects of the interaction between primary osteogenic cells derived from newborn rat calvariae and Ti surfaces with nanotopography [de Oliveira and Nanci, 2004; de Oliveira et al., 2007; Bueno et al., 2011]. The expression of bone matrix proteins such as bone sialoprotein (Bsp) is upregulated by this nanotopography at early phases of the culture progression [de Oliveira and Nanci, 2004]. Additionally, it has been observed that the nanotopography design is etching time dependent and that the extracellular osteopontin (Opn) deposition is higher on Ti surfaces treated for 4 h compared with 30 min [Bueno et al., 2011]. Despite our encouraging outcomes, the mechanisms involved in the osteogenic potential of this nanopattern has not yet been fully explored and understood. Thus, here we have investigated the osteoinductive ability of our Ti with nanotopography surface, which potentiates the rat MSCs differentiation toward an osteoblast lineage in the absence of osteoinductive factors and suggested a novel nanotopography regulated integrin signaling mechanism involved in this phenomenon.

MATERIALS AND METHODS

TI SURFACES PREPARATION

Discs of commercially pure grade 2 Ti, with 12 mm in diameter and 1.5 mm thick, were polished using 320 and 600 grit silicon carbide, cleaned by sonication and rinsed with toluene. Samples were treated with a blend of 10 N H_2SO_4 and 30% aqueous H_2O_2 (1:1 v/v) for 4 h at room temperature under continuous agitation to produce the surface nanotopography [Yi et al., 2006]. Treated and untreated (control) Ti discs were rinsed with deionized H_2O, autoclaved and air-dried. The surfaces were examined using a field emission scanning electron microscope (Inspect S50, FEI, Hillsboro, OR) operated at 5 kV.

CELL CULTURE

Bone marrow was obtained from femora of 5-week male Wistar rats (120–150 g) under the regulation of the Committee of Ethics in Animal Research of the University of Sao Paulo and plated into culture flasks containing growth medium, that is, alpha-minimum essential medium (α-MEM—Invitrogen-Life Technologies, Grand Island, NY) supplemented with 10% fetal calf serum (Gibco-Life Technologies), 50 μg/ml gentamycin (Gibco-Life Technologies) and 0.3 μg/ml fungisone (Gibco-Life Technologies). MSCs were selected by adherence to polystyrene and expanded in the same medium until subconfluence. First passage cells were cultured in 24-well culture plates on Ti with nanotopography and control Ti discs at a cell density of 2×10^4 cells/disc in either growth medium or osteogenic medium, which was growth medium with addition of 5 μg/ml ascorbic acid (Gibco-Life Technologies), 7 mM β-glycerophosphate (Sigma-Aldrich) and 10^{-7} M dexamethasone (Sigma-Aldrich, St. Louis, MO) for periods of up to 21 days. Cultures were kept at 37°C in a humidified atmosphere of 5% CO_2 and 95% air; the medium was changed three times a week.

CELL COUNTING

Cells grown in osteogenic medium on Ti with nanotopography and control Ti discs for periods of 4, 10, and 17 days were enzymatically detached from Ti discs using 1 mM EDTA, 1.3 mg/ml collagenase, and 0.25% trypsin solution (Gibco-Life Technologies). The total number of cells/disc, and the percentage of viable and nonviable cells were determined after Trypan blue (Sigma-Aldrich) staining using an automated cell counter (Invitrogen-Life Technologies).

ALKALINE PHOSPHATASE (ALP) ACTIVITY

At days 4, 10, and 17 the release of thymolphthalein from thymolphthalein monophosphate was determined to measure the Alp activity of cells grown in osteogenic medium on Ti with nanotopography and control Ti discs using a commercial kit (Labtest Diagnostica SA, Belo Horizonte, MG, Brazil). A mixture of 50 μl of thymolphthalein monophosphate and 0.5 ml of 0.3 M diethanolamine buffer, pH 10.1 was kept for 2 min at 37°C. Then, 50 μl of the cell lysates obtained by five cycles of thermal shock (−20°C for 20 min, and 37°C for 15 min) from each Ti disc were added and, after 10 min at 37°C 2 ml of a solution of Na_2CO_3 (0.09 mmol/ml) and NaOH (0.25 mmol/ml) were used to stop the reaction. The absorbance was measured at 590 nm in the plate reader μQuant (Biotek, Winooski, VT) and Alp activity was expressed as μmol thymolphthalein normalized by the total number of cells at the respective time-point.

EXTRACELLULAR MATRIX MINERALIZATION

At day 21, cells grown in osteogenic medium on Ti with nanotopography and control Ti discs were fixed in 10% formalin for 2 h at room temperature, dehydrated and stained with 2% Alizarin Red S (Sigma-Aldrich), pH 4.2, for 10 min. The discs were then observed by fluorescence microscopy (Axio Imager M2, Carl Zeiss, Göttingen, Germany) outfitted with an Axiocam MRm digital camera under epifluorescence and the acquired images were processed with Axiovision 4.8.2 image processing and analysis system. The calcium content was detected using a colorimetric method. Succinctly, 280 μl of 10% acetic acid were added to each well and the plate was incubated at room temperature for 30 min under shaking. This solution was vortexed for 1 min, heated to 85°C for 10 min, and transferred to ice for 5 min. The slurry was centrifuged at 13,000*g* for 15 min and 100 μl of the supernatant was mixed with 40 μl of 10% ammonium hydroxide and this solution was spectrophotometrically read at 405 nm in the plate reader μQuant (Biotek) and the data were expressed as absorbance.

GENE EXPRESSION OF THE KEY BONE MARKERS

Quantitative real-time PCR was carried out at day 10 to evaluate the gene expression of runt-related transcription factor 2 (Runx2), collagen type I alpha 1 (ColIA1), Alp, osteocalcin (Oc), Bsp, and bone morphogenetic protein 4 (Bmp-4) in cells grown in osteogenic medium on Ti with nanotopography and control Ti discs. The total RNA was extracted with Trizol reagent (Invitrogen-Life Technologies) according to the manufacturer's instructions. The concentration and purity of RNA samples were determined by optical density at a wavelength of 260 and 260:280 nm, respectively and only samples presenting 260:280 ratios higher than 1.8 were analyzed. Complementary DNA (cDNA) was synthesized using 1 μg of the RNA through a reverse transcription reaction (M-MLV reverse transcriptase, Promega Corporation, Madison, WI). Real-time PCR was carried out in a CFX96 Real-Time PCR Detection System (Bio-Rad Laboratories, Philadelphia, PA) using SybrGreen PCR Master-Mix

(Applied Biosystems, Foster City, CA), specific primers (Table I) designed with Primer Express 2.0 (Applied Biosystems) and 12.5 ng of cDNA. The relative gene expressions were normalized to β-actin expression and the real changes were expressed relative to the control Ti discs using the cycle threshold method.

EFFECT OF THE TI WITH NANOPOGRAPHY SURFACE ON THE OSTEOBLAST DIFFERENTIATION OF MSCs

In order to investigate whether Ti with nanotopography surface can affect gene expression of the key bone markers by itself, cells were expanded in growth medium until subconfluence. Thus, they were seeded on Ti with nanotopography and control Ti discs and again cultured in growth medium, which means in the absence of the osteogenic factors, ascorbic acid (Gibco-Life Technologies), β-glycerophosphate (Sigma-Aldrich) and dexamethasone (Sigma-Aldrich). At day 10, the gene expression of Runx2, ColIA1, Alp, Oc, Bsp, and Bmp-4 was evaluated by quantitative real-time PCR.

ROLE OF α1β1 INTEGRIN ON THE OSTEOINDUCTIVE EFFECT OF TI WITH NANOPOGRAPHY SURFACE

As a first step, cells were expanded in growth medium until subconfluence and afterwards seeded on Ti with nanotopography and control Ti discs and again cultured in growth medium. At day 10, the gene expression of α1β1 integrin was evaluated by quantitative real-time PCR. Secondly, cells were expanded in growth medium until subconfluence and then seeded only on Ti with nanotopography discs and cultured in growth medium in presence of either 10 nM obtustatin, a potent selective inhibitor of α1β1 integrin, or vehicle (distilled water) for periods of up to 10 days [Marcinkiewicz et al., 2003]. Thus, at 24 h, cell adhesion and spreading, and the presence of Opn were evaluated by fluorescence labeling. At day 10, we evaluated the gene expression of the same key bone markers mentioned above by quantitative real-time PCR and Alp activity.

FLUORESCENCE LABELING

To evaluate cell adhesion and morphology, and the presence of Opn, cells were cultured on Ti with nanotopography discs in growth medium in presence of either 10 nM obtustatin or vehicle for 24 h. Then, the cells were fixed with 4% paraformaldehyde in 0.1 M phosphate buffer (PB), pH 7.2, for 10 min at room temperature. Cell permeabilization was carried out using 0.5% Triton X-100 (Acros Organics, Geel, Belgium) in PB for 10 min followed by blocking with 5% skimmed milk in PB for 30 min. A primary monoclonal antibody to Opn (MPIIIB10-1, 1:800; Developmental Studies Hybridoma Bank, Iowa City, IA) was used, followed by a mixture of Alexa Fluor 594 (red fluorescence) conjugated goat anti-mouse secondary antibody (1:200, Molecular Probes, Eugene, OR) and Alexa Fluor 488 (green fluorescence) conjugated phalloidin (1:200, Molecular Probes) for the detection of actin cytoskeleton (60 min each antibody). Cell nuclei were stained with 300 nM 4′,6-diamidino-2-phenylindole, dihydrochloride (DAPI, Molecular Probes) for 5 min and a glass coverslip was mounted with an antifade kit (Prolong; Molecular Probes) on the Ti surface containing cells. The samples were examined under epifluorescence as described above and the acquired digital images were processed with Adobe Photoshop software (Adobe Systems, San Jose, CA).

STATISTICAL ANALYSIS

The data presented in this work are the representative results of three independent experiments using three sets of cultures established from three different pools of rats. For each experiment, cell counting, Alp activity and extracellular matrix mineralization were carried out in quadruplicates ($n = 4$), and gene expression, in triplicates ($n = 3$). The numerical data of Ti with nanotopography were compared with control Ti surface by Mann–Whitney U test and the level of significance was set at 5%. Comparisons of cells grown on Ti with nanotopography in presence of either obtustatin or vehicle were also done by Mann–Whitney U test using the same level of significance.

RESULTS

At the microscale, control and Ti nanotopography surfaces presented similar topography with multidirectional groves (Fig. 1A,B). Under higher magnification, and therefore at the nanoscale, control Ti showed a smooth surface while Ti with nanotopography exhibited a network of nanopits (Fig. 1C,D). A progressive increase in the cell number was noticed on Ti with nanotopography during the entire time-course, from days 0 to 17, while on control Ti, culture growth reached a plateau at day 10 (Fig. 2A). Besides, the number of cells was higher on Ti with nanotopography than on control Ti at days 10 ($P = 0.07$) and 17 ($P = 0.03$), without statistically significant difference ($P = 0.27$) at day 4 (Fig. 2A). On both, Ti with nanotopography and control Ti, Alp activity peaked at day 10 (Fig. 2B). The surface

TABLE I. Primer Sequences and Product Size (bp) for Real-Time PCR Reactions

Gene	Sense sequence anti-sense sequence	bp
Runx2	CACAAACAACCACAGAACCAC TTGCTGTCCTCCTGGAGAAA	56
ColIA1	CCAACGAGATCGAGCTCAGG GACTGTCTTGCCCCAAGTTCC	101
Alp	CCAACTCATTTGTGCCAGAG CAGGGCATTTTTCAAGGTCTC	80
Oc	GCAGACACCATGAGGACCCT CCGGAGTCTATTCACCACCTTACTG	153
Bsp	CTACTTTTATCCTCCTCTGAAACGGTT GCTAGCGGTTACCCCTGAGA	202
Bmp-4	CGCAGCTTCTCTGAGCCTTTCCA ACGACCATCAGCATTCGGTTACCAG	127
α1 Integrin	GCAACCGGAAGCGAGAGCTGG TAGCAGCAGTAGCCCCGCGA	107
β1 Integrin	GCAGGCGTGGTTGCCGGAAT TTTTCACCCGTGTCCCACTTGGC	140
β-Actin	AAATGCTTCTAGGCGGACTG GGTTTTGTCAAAGAAAGGGTG	59

Runt-related transcription factor 2 (Runx2), collagen type I alpha 1 (ColIA1), alkaline phosphatase (Alp), osteocalcin (Oc), bone sialoprotein (Bsp), bone morphogenetic protein 4 (Bmp-4).

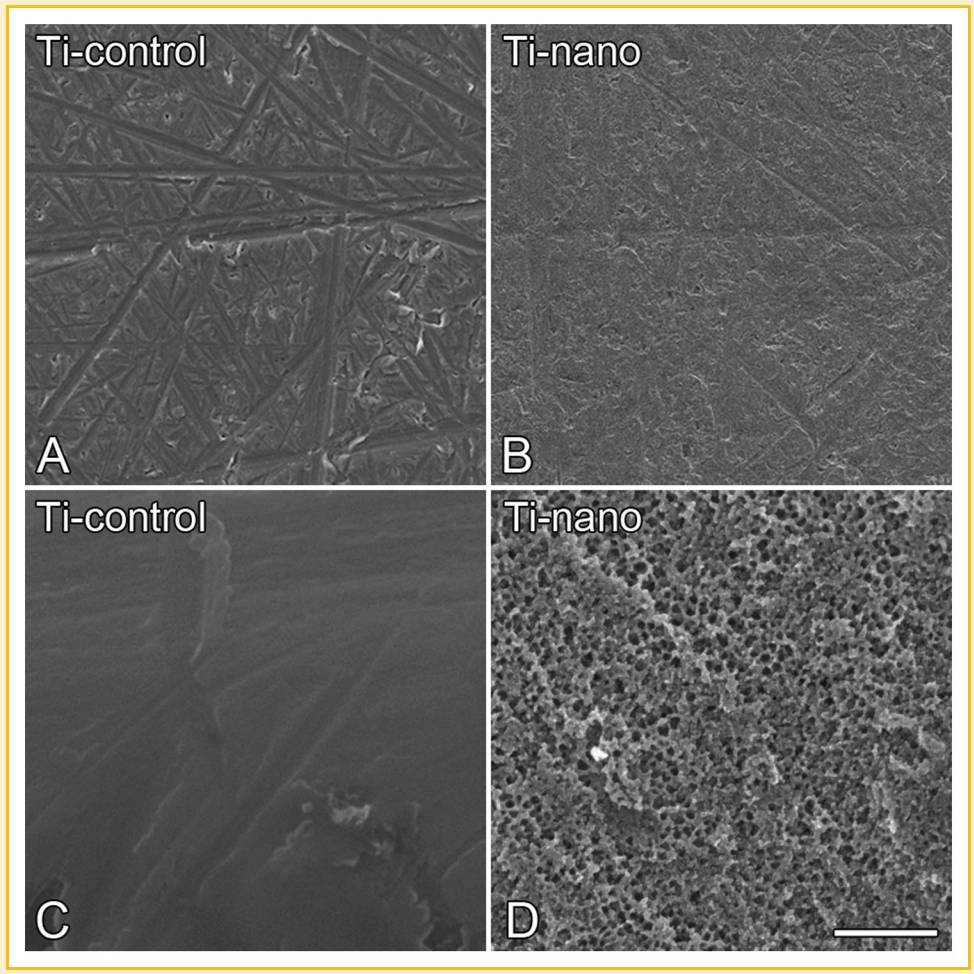

Fig. 1. High resolution scanning electron micrographs of control (A,C) and nanotopography (B,D) Ti surfaces. Both Ti surfaces exhibit similar topography with multidirectional groves at lower magnification (A,B). Under higher magnification, control Ti presents a smooth surface while Ti with nanotopography exhibits a network of nanopits (C,D). Scale bar: A,B = 50 μm and C,D = 1 μm.

with nanotopography supported higher Alp activity at days 4 ($P = 0.01$) and 10 ($P = 0.04$) and it was statistically the same ($P = 0.35$) at day 17 (Fig. 2B). After 21 days in culture, we detected the presence of mineralized matrix on both surfaces without statistically significant difference ($P = 0.13$) in the amount of calcium between Ti with nanotopography and control Ti surfaces (Fig. 2C). At day 10, it was found a higher expression of all evaluated genes, Runx2 ($P = 0.001$, $P = 0.0006$), ColIA1 ($P = 0.01$, $P = 0.0002$), Alp ($P = 0.01$, $P = 0.007$), Oc ($P = 0.003$, $P = 0.00001$), Bsp ($P = 0.05$, $P = 0.0002$), and Bmp-4 ($P = 0.0003$, $P = 0.0001$) on Ti with nanotopography compared with control Ti under both osteogenic and non-osteogenic conditions, respectively (Fig. 3A,B). Qualitatively cell adhesion and morphology and Opn expression were not affected by obtustatin at 24 h (Fig. 4). Ti with nanotopography supported cell adhesion and spreading, which were mainly stellate-shaped either in presence of vehicle or obtustatin (Fig. 4A,B). In cells grown in non-osteogenic medium for 10 days, the gene expression of $\alpha 1$ and $\beta 1$ integrins was higher ($P = 0.0005$ and $P = 0.00005$, respectively) on Ti with nanotopography than on control Ti (Fig. 5A). At day 10, the use of obtustatin downregulated the gene expression of ColIA1 ($P = 0.02$), Alp ($P = 0.003$), Oc ($P = 0.05$), Bsp ($P = 0.001$), and Bmp-4 ($P = 0.003$), without affecting Runx2 ($P = 0.45$; Fig. 5B). Furthermore, obtustatin reduced the Alp activity ($P = 0.003$) (Fig. 5C) in cultures grown on Ti with nanotopography surface under non-osteogenic condition.

DISCUSSION

The results of our study show that under standard osteogenic condition the Ti with nanopotography surface favors cell proliferation and enhances osteoblast differentiation of MSCs evidenced by higher Alp activity and increased gene expression of key bone markers. We also noticed the development of the microenvironment to architect osteoblast phenotype in MSCs grown on Ti with nanotopography surface in the absence of osteoinductor factors.

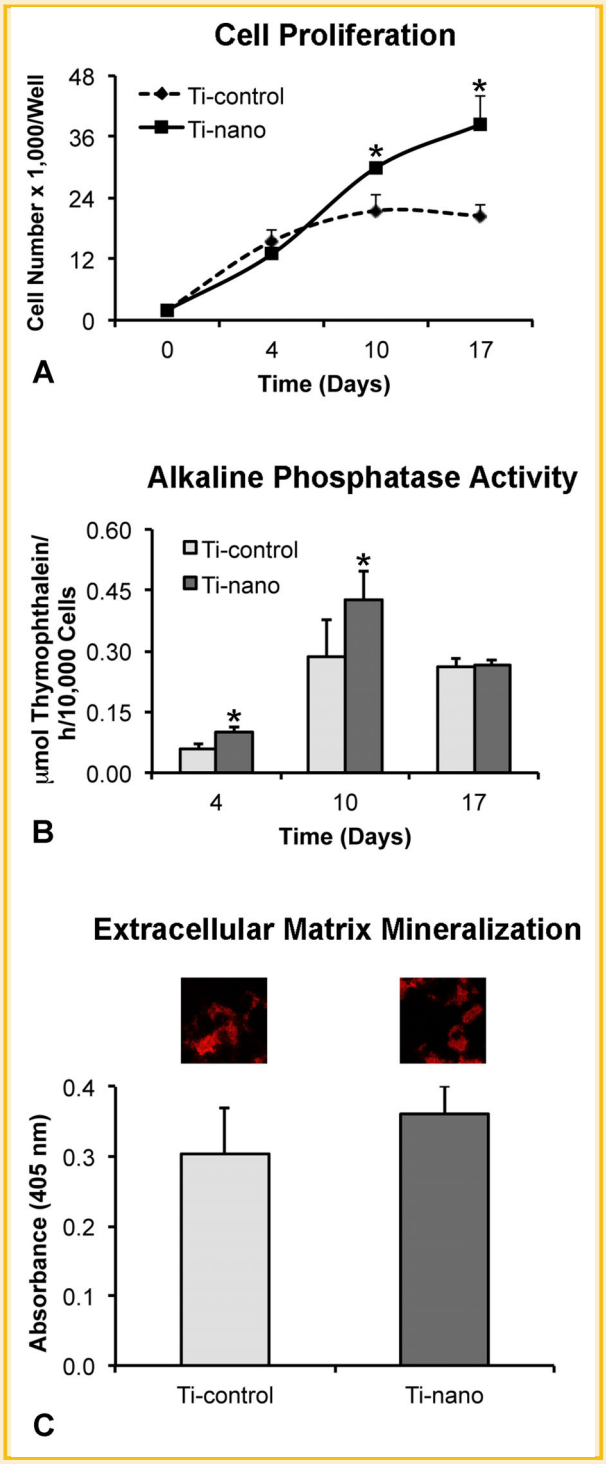

Fig. 2. Proliferation (A), alkaline phosphatase (Alp) activity (B), and extracellular matrix mineralization (C) of MSCs differentiated into osteoblasts and cultured on nanotopography and control Ti surfaces in an osteogenic medium. The number of cells was higher on Ti with nanotopography on days 10 ($P=0.07$) and 17 ($P=0.03$) (A). Ti surface with nanotopography supported higher Alp activity on days 4 ($P=0.01$) and 10 ($P=0.04$) (B). The amount of calcium in the mineralized matrix (insets) was not statistically significant different ($P=0.13$) by comparing both surfaces (C). The data are presented as mean ± standard deviation (n = 4). *Indicates statistically significant difference.

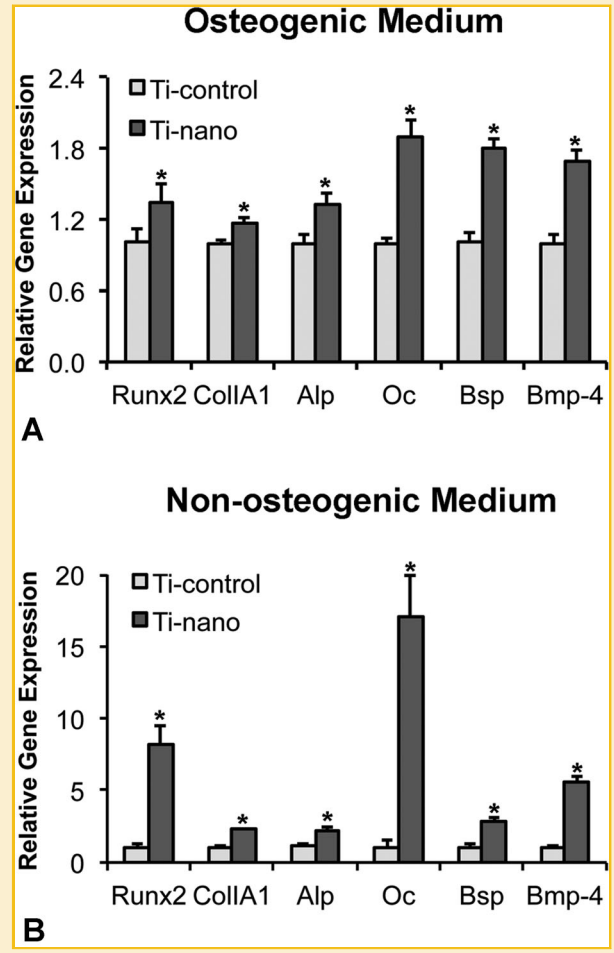

Fig. 3. Gene expression of bone markers of MSCs cultured on nanotopography and control Ti surfaces in an osteogenic (A) and non-osteogenic (B) medium at day 10. A higher expression of Runx2 ($P=0.001$ and $P=0.0006$), ColIA1 ($P=0.01$ and $P=0.0002$), Alp ($P=0.01$ and $P=0.007$), Oc ($P=0.03$ and $P=0.00001$), Bsp ($P=0.05$ and $P=0.0002$), and Bmp-4 ($P=0.003$ and $P=0.0001$) was noticed on Ti with nanotopography surface under both osteogenic (A) and non-osteogenic (B) conditions, respectively. The data are presented as mean ± standard deviation (n = 3). *Indicates statistically significant difference.

Finally, by using obtustatin, we demonstrated that α1β1 integrin signaling pathway determines, at least in part, the osteoinductive effect of nanotopography on MSCs.

Succeeding cellular adhesion and aiming at colonizing implant surface, cells start to proliferate and it has been reported a higher proliferation rate in MC3T3-E1 preosteoblastic cells as well as cells derived from newborn rat calvariae grown on Ti with nonotopography [de Oliveira et al., 2007; Vetrone et al., 2009]. In keeping with these, here, we observed that Ti with nanotopography surface promoted a profound increase in the total cell number count on days 10 and 17 compared with control Ti surface. To track the culture progression through the osteoblast differentiation we analyzed the Alp activity, an enzyme, which plays a primary role in the mineralization phenomenon [Beck et al., 1998]. A typical curve of

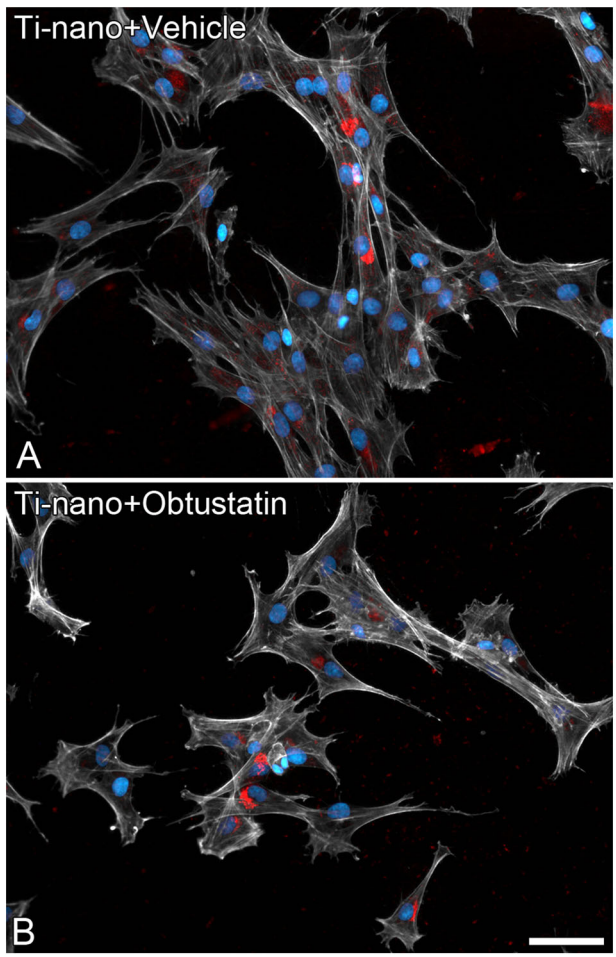

Fig. 4. Epifluorescence of MSCs cultured on Ti with nanotopography in a non-osteogenic medium either in presence of vehicle (A) or obtustatin (B) at 24 h. Green fluorescence, which appears in pale white, reveals the actin cytoskeleton, blue fluorescence indicates cell nuclei and osteopontin (Opn) is shown in red. Qualitatively, no major differences were detected between both vehicle and obtustatin in terms of cell adhesion, morphology and Opn expression. Scale bar = 100 μm.

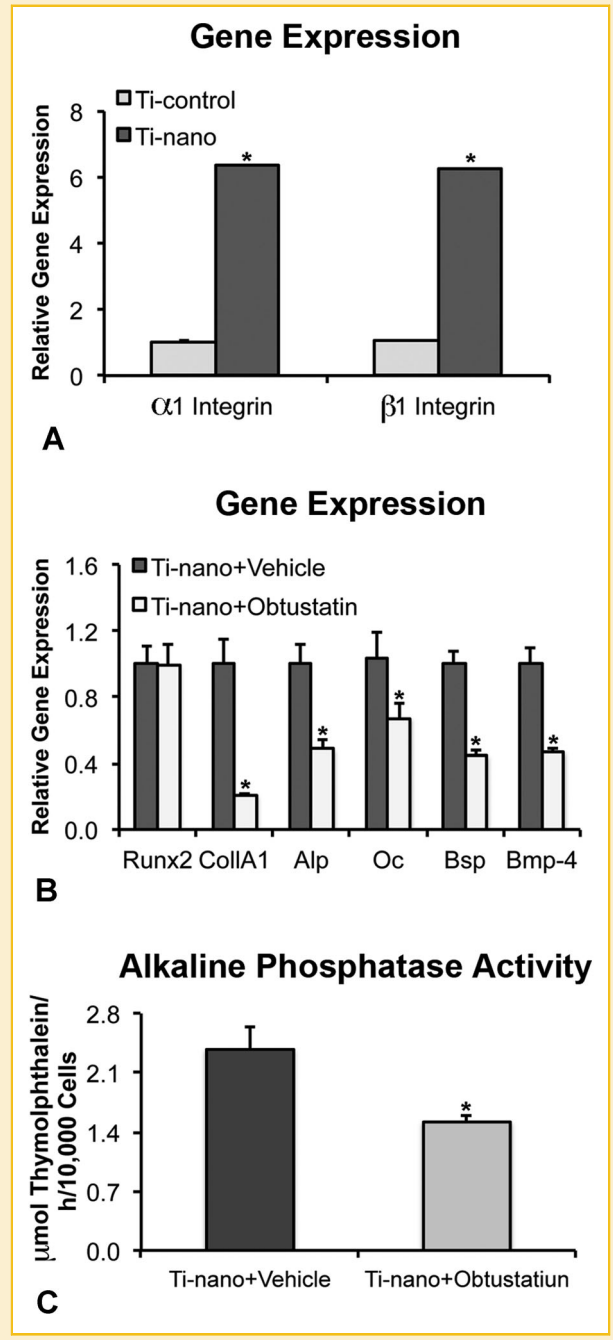

Fig. 5. The role of $\alpha 1\beta 1$ integrin on osteoblast differentiation of MSCs induced by Ti with nanotopography in a non-osteogenic medium. Gene expression of $\alpha 1\beta 1$ integrin of MSCs cultured on nanotopography and control Ti surfaces at day 10 (A). A higher expression of $\alpha 1$ and $\beta 1$ integrins ($P = 0.00001$ for both) was noticed on Ti with nanotopography surface. Effect of obtustatin on the gene expression of bone markers (B) and on alkaline phosphatase (Alp) activity (C) of MSCs cultured on Ti with nanotopography surface at day 10. The obtustatin downregulated the gene expression of CollA1 ($P = 0.018$), Alp ($P = 0.003$), Oc ($P = 0.05$), Bsp ($P = 0.001$), and Bmp-4 ($P = 0.003$) and reduced Alp activity ($P = 0.003$). The data are presented as mean ± standard deviation ($n = 3$ for gene expression and $n = 4$ for Alp activity). *Indicates statistically significant difference.

Alp activity peaking at day 10 as described elsewhere was noticed for both Ti surfaces and nanotopography allowed a higher activity at days 4 and 10 [de Oliveira et al., 2007]. It is note worthy to mention that the high Alp activity did not lead to a higher extracellular matrix mineralization on the Ti with nanotopography surface, opposite to previous observation using cells derived from newborn rat calvariae grown on the same substrate [de Oliveira et al., 2007]. The differences in the sensitivity of the methods employed and the use of MSCs, a less differentiated culture model compared with calvariae derived cells, could explain the lack of differences between nanotopography and control Ti surfaces in terms of extracellular matrix mineralization.

In an attempt to further investigate the osteoblast features of MSCs, we examined the gene expression of Runx2, ColIA1, Alp, Oc, Bsp, and Bmp-4, the key bone markers expressed at different stages of osteoblast differentiation. Runx2 is a master regulator of bone

formation and ColIA1 is the main protein of the extracellular bone matrix while its fibrils are the source of tensile strength [Canty and Kadler, 2005; Komori et al., 1997]. Bsp and Oc are non-collagenous matrix proteins, which are involved in the nucleation of hydroxyapatite crystals and modulation of the mineralization, respectively [Owen et al., 1990; Gams et al., 1999]. Bmp-4, an osteogenic protein, is able to induce ectopic bone formation [Reddi and Cunningham, 1993]. Our outcomes showed that all osteoblast marker genes were upregulated in cells grown on Ti with nanotpography compared with control Ti surface at least in one (10 days) of the three evaluated time-points (4 and 17 days are not shown). Corroborating our findings, it has been shown that nanotopography generated by aluminium oxide nanocoating also leads to an increase in the gene expression representative of the osteoblast differentiation in human MSCs grown on Ti surface [Mendonça et al., 2009].

Among different Ti nanostructures, TiO_2 nanotubes have been the target of many recent studies and it has been displayed that the size of the nanotubes may dictate the cell fate [Brammer et al., 2009; Oh et al., 2009; Park et al., 2009; Yu et al., 2010; Zhang et al., 2011]. More specifically, nanotubes ranging from 70- to 100-nm diameter induce osteoblast differentiation of human MSCs in the absence of osteoinductive factors [Oh et al., 2009]. Also, polyurethane surfaces exhibiting submicron patterned ridges and grooves elicit the same effect on human MSCs [Watari et al., 2012]. As Ti with nanotopography surface increased the expression of all evaluated genes on day 10 in an osteogenic milieu, we highlighted this time-point to address the hypothesis that our nanotopography by itself can affect osteoblast differentiation. Our results pointed out that this Ti with nanotpography surface induces the gene expression of all evaluated bone markers when cells were grown in a non-osteogenic medium. Interestingly, the increase in gene expression induced by Ti with nanotpography was more pronounced in a non-osteogenic environment, suggesting that the osteoinductor factors presented in the osteogenic medium could mask the effect of nanotopography.

The uniqueness of nanotopography is its ability to mimic the extracellular matrix (ECM) [Wang, 2003; Tran and Webster, 2009]. It is well known that integrins, a large family of cell surface receptors, mediate cell–ECM interactions [Siebers et al., 2005] that exert a key role on cellular adhesion, migration, proliferation and differentiation during bone development and repair [Ekholm et al., 2002; Allori et al., 2008]. Thus, our investigation was focused on integrins, specifically $\alpha 1\beta 1$ integrin, which are associated with the bone repair process disruption, as being one of the signaling pathways triggered by the nanotopography to induce osteoblast differentiation. Our outcomes showed a dramatic increase in the gene expression of $\alpha 1\beta 1$ integrin in MSCs grown on nanotopography compared with control Ti surface in a non-osteogenic medium. To demonstrate that nanotopography drives MSCs fate toward osteoblast differentiation through $\alpha 1\beta 1$ integrin signaling pathway, we cultured MSCs on Ti with nanotopography surface in presence of obtustatin, a potent selective inhibitor of $\alpha 1\beta 1$ integrin

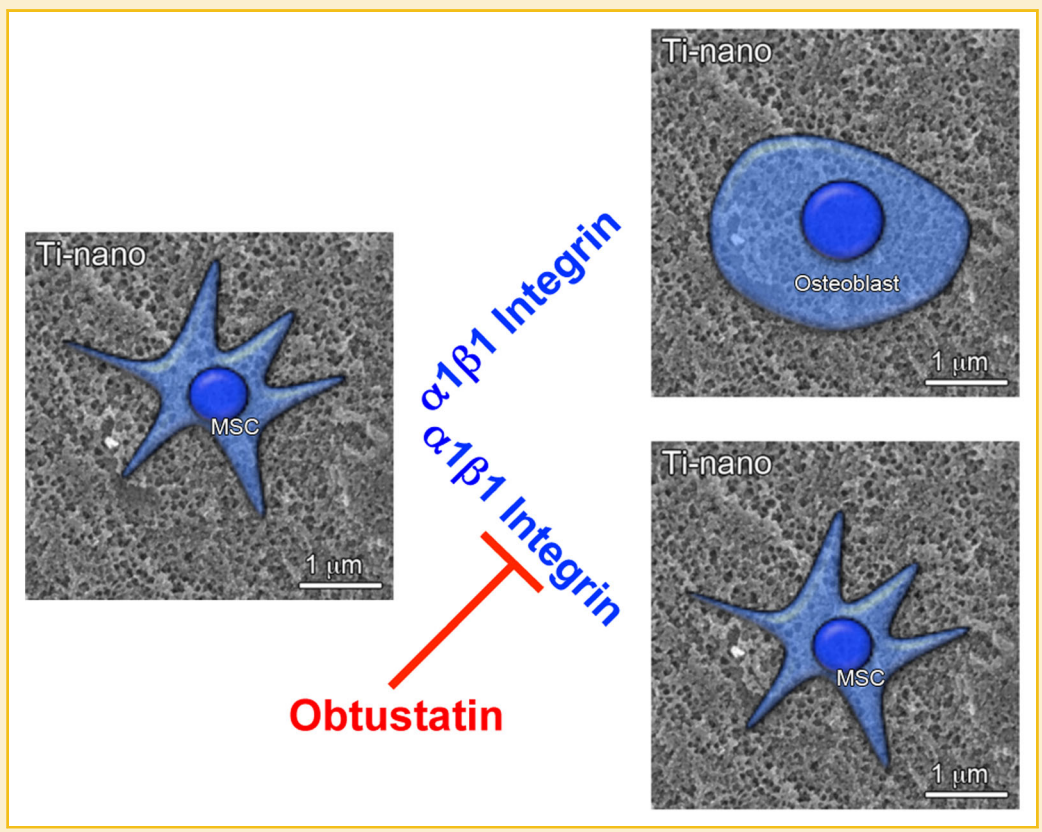

Fig. 6. Schematic representation of the key role of $\alpha 1\beta 1$ integrin on osteoblast differentiation of MSCs induced by Ti with nanotopography surface.

[Marcinkiewicz et al., 2003]. Our findings clearly showed that the higher gene expression of bone markers and Alp activity induced by nanotopography was inhibited by obtustatin, disclosing the central role of $\alpha 1\beta 1$ integrin on osteoblast differentiation induced by nanotopography (Fig. 6).

In conclusion, we have shown that the association of physical (e.g.: presence of nanopits) and chemical (e.g., TiO_2 layer thickness and purity) modifications of Ti surface produced by oxidation using a mixture of H_2SO_4/H_2O_2 of Ti increases cell proliferation and osteoblast differentiation in an osteogenic medium. We have also noticed that this nanotopography drives MSCs differentiation toward the osteoblast lineage in the absence of osteogenic factors. To our knowledge, this is the first report indicating that $\alpha 1\beta 1$ integrin signaling pathway determines the osteoinductive effect of this Ti with nanotopography surface on MSCs. This finding sheds light on a novel mechanism involved in nanosurface-mediated MSCs fate and is a major step in the development of new surface modifications aiming to accelerate and/or enhance the process of osseointegration.

ACKNOWLEDGEMENTS

We would like to thank Roger R. Fernandes and Milla S. Tavares for the assistance they provided during the cell culture experiments and Lubana Afreen for editing the manuscript.

REFERENCES

Allori AC, Sailon AM, Warren SM. 2008. Biological basis of bone formation, remodeling, and repair-part II: Extracellular matrix. Tissue Eng Part B Rev 14:275–283.

Beck GR, Jr., Sullivan EC, Moran E, Zerler B. 1998. Relationship between alkaline phosphatase levels, osteopontin expression, and mineralization in differentiating MC3T3-E1 osteoblasts. J Cell Biochem 68:269–280.

Brammer KS, Oh S, Cobb CJ, Bjursten LM, van der Heyde H, Jin S. 2009. Improved bone-forming functionality on diameter-controlled TiO_2 nanotube surface. Acta Biomater 5:3215–3223.

Bueno RB, Adachi P, Castro-Raucci LM, Rosa AL, Nanci A, de Oliveira PT. 2011. Oxidative nanopatterning of titanium surfaces promotes production and extracellular accumulation of osteopontin. Braz Dent J 22:179–184.

Canty EG, Kadler KE. 2005. Procollagen trafficking, processing and fibrillogenesis. J Cell Sci 118:1341–1353.

de Oliveira PT, Nanci A. 2004. Nanotexturing of titanium-based surfaces upregulates expression of bone sialoprotein and osteopontin by cultured osteogenic cells. Biomaterials 25:403–413.

de Oliveira PT, Zalzal SF, Beloti MM, Rosa AL, Nanci A. 2007. Enhancement of in vitro osteogenesis on titanium by chemically produced nanotopography. J Biomed Mater Res A 80:554–564.

Dimitrievska S, Bureau MN, Antoniou J, Mwale F, Petit A, Lima RS, Marple BR. 2011. Titania-hydroxyapatite nanocomposite coatings support human mesenchymal stem cells osteogenic differentiation. J Biomed Mater Res A 98:576–588.

Divya Rani VV, Manzoor K, Menon D, Selvamurugan N, Nair SV. 2009. The design of novel nanostructures on titanium by solution chemistry for an improved osteoblast response. Nanotechnology 20:195101–195111.

Ekholm E, Hankenson KD, Uusitalo H, Hiltunen A, Gardner H, Heino J, Penttinen R. 2002. Diminished callus size and cartilage synthesis in alpha 1 beta 1 integrin-deficient mice during bone fracture healing. Am J Pathol 160:1779–1785.

Gams B, Kim RH, Sodek J. 1999. Bone sialoprotein. Crit Rev Oral Biol Med 10:79–98.

Gittens RA, Olivares-Navarrete R, Cheng A, Anderson DM, McLachlan T, Stephan I, Geis-Gerstorfer J, Sandhage KH, Fedorov AG, Rupp F, Boyan BD, Tannenbaum R, Schwartz Z. 2013. The roles of titanium surface micro/nanotopography and wettability on the differential response of human osteoblast lineage cells. Acta Biomater 9:6268–6277.

Komori T, Yagi H, Nomura S, Yamaguchi A, Sasaki K, Deguchi K, Shimizu Y, Bronson RT, Gao YH, Inada M, Sato M, Okamoto R, Kitamura Y, Yoshiki S, Kishimoto T. 1997. Targeted disruption of Cbfa1 results in a complete lack of bone formation owing to maturational arrest of osteoblasts. Cell 89: 755–764.

Marcinkiewicz C, Weinreb PH, Calvete JJ, Kisiel DG, Mousa SA, Tuszynski GP, Lobb RR. 2003. Obtustatin: A potent selective inhibitor of alpha1beta1 integrin in vitro and angiogenesis in vivo. Cancer Res 63:2020–2023.

Mendonça G, Mendonça DB, Simões LG, Araújo AL, Leite ER, Duarte WR, Aragão FJ, Cooper LF. 2009. The effects of implant surface nanoscale features on osteoblast-specific gene expression. Biomaterials 30:4053–4062.

Mendonça G, Mendonça DB, Aragão FJ, Cooper LF. 2010. The combination of micron and nanotopography by H(2)SO(4)/H(2)O(2) treatment and its effects on osteoblast-specific gene expression of hMSCs. J Biomed Mater Res A 94:169–179.

Menon D, Divyarani VV, Lakshmanan VK, Anitha VC, Koyakutty M, Nair SV. 2012. Osteointegration of titanium implant is sensitive to specific nanostructure morphology. Acta Biomater 8:1976–1989.

Oh S, Brammer KS, Li YS, Teng D, Engler AJ, Chien S, Jin S. 2009. Stem cell fate dictated solely by altered nanotube dimension. Proc Natl Acad Sci USA 106:2130–2135.

Owen T, Aronow M, Shalhoub V, Barone L, Wilming LM, Tassinari MS, Kennedy MB, Pockwinse S, Lian JB, Stein GS. 1990. Progressive development of the rat phenotype in vitro: Reciprocal relationships in expression of genes associated with osteoblast proliferation and differentiation during formation of the bone extracellular matrix. J Cell Physiol 143:420–430.

Park J, Bauer S, Schlegel KA, Neukam FW, von der Mark K, Schmuki P. 2009. TiO_2 nanotube surfaces: 15 nm—An optimal length scale of surface topography for cell adhesion and differentiation. Small 5:666–671.

Raimondo T, Puckett S, Webster TJ. 2010. Greater osteoblast and endothelial cell adhesion on nanostructured polyethylene and titanium. Int J Nanomedicine 5:647–652.

Reddi AH, Cunningham NS. 1993. Initiation and promotion of bone differentiation by bone morphogenetic proteins. J Bone Miner Res 8(Suppl 2): S499–S502.

Siebers MC, ter Brugge PJ, Walboomers XF, Jansen JA. 2005. Integrins as linker proteins between osteoblasts and bone replacing materials. A critical review. Biomaterials 26:137–146.

Tran N, Webster TJ. 2009. Nanotechnology for bone materials. Wiley Interdiscip Rev Nanomed Nanobiotechnol 1:336–351.

Variola F, Yi J-H, Richert L, Wuest JD, Rosei F, Nanci A. 2008. Tailoring the surface properties of Ti6Al4V by controlled chemical oxidation. Biomaterials 29:1285–1298.

Vetrone F, Variola F, Tambasco de Oliveira P, Zalzal SF, Yi JH, Sam J, Bombonato-Prado KF, Sarkissian A, Perepichka DF, Wuest JD, Rosei F, Nanci A. 2009. Nanoscale oxidative patterning of metallic surfaces to modulate cell activity and fate. Nano Lett 9:659–665.

Wang M. 2003. Developing bioactive composite materials for tissue replacement. Biomaterials 24:2133–2151.

Ward BC, Webster TJ. 2006. The effect of nanotopography on calcium and phosphorus deposition on metallic materials in vitro. Biomaterials 27: 3064–3074.

Watari S, Hayashi K, Wood JA, Russell P, Nealey PF, Murphy CJ, Genetos DC. 2012. Modulation of osteogenic differentiation in hMSCs cells by submicron topographically-patterned ridges and grooves. Biomaterials 33:128–136.

Yi J-H, Bernard C, Variola F, Zalzal SF, Wuest JD, Rosei F, Nanci A. 2006. Characterization of a bioactive nanotextured surface created by controlled chemical oxidation of titanium. Surf Sci 600:4613–4621.

Yu WQ, Jiang XQ, Zhang FQ, Xu L. 2010. The effect of anatase TiO_2 nanotube layers on MC3T3-E1 preosteoblast adhesion, proliferation, and differentiation. J Biomed Mater Res A 94:1012–1022.

Zhang Z, Sun J, Hu H, Wang Q, Liu X. 2011. Osteoblast-like cell adhesion on porous silicon-incorporated TiO2 coating prepared by micro-arc oxidation. J Biomed Mater Res B Appl Biomater 97:224–234.